Applied Catalysis B: Environmental 96 (2010) 142–147

Contents lists available at ScienceDirect

Applied Catalysis B: Environmental

journal homepage: www.elsevier.com/locate/apcatb

Characterization of Cr(III)-grafted TiO_2 for photocatalytic reaction under visible light

Hiroshi Irie [a,*], Toshihiko Shibanuma [b], Kazuhide Kamiya [b], Shuhei Miura [b], Toshihiko Yokoyama [c], Kazuhito Hashimoto [b,d,**]

[a] Clean Energy Research Center, University of Yamanashi, 4-3-11 Takeda, Kofu, Yamanashi 400-8511, Japan
[b] Department of Applied Chemistry, School of Engineering, The University of Tokyo, 7-3-1 Hongo, Bunkyo-ku, Tokyo 113-8656, Japan
[c] Institute for Molecular Science, Myodaiji-cho, Okazaki, Aichi 444-8585, Japan
[d] Research Center for Advanced Science and Technology, The University of Tokyo, 4-6-1 Komaba, Meguro-ku, Tokyo 153-8904, Japan

ARTICLE INFO

Article history:
Received 10 December 2009
Received in revised form 4 February 2010
Accepted 4 February 2010
Available online 11 February 2010

Keywords:
Photocatalysis
Visible light
Cr(III) ion
TiO_2
Oxidative decomposition

ABSTRACT

We investigated the chemical state and environment of Cr ions in a Cr ion-grafted TiO_2 photocatalyst by means of X-ray absorption fine structure (XAFS) measurements. The XAFS results indicated that the Cr ions exist on TiO_2 as Cr(III) in an amorphous Cr_2O_3-like structure. The Cr_2O_3-like structure formed clusters and attached to the TiO_2 surface. The activity (CO_2 generation rate and QE value) was evaluated by 2-propanol decomposition under visible light (1 mW cm^{-2}, 450–580 nm) and was highest with a weight fraction of Cr/TiO_2 equaling 1.0×10^{-3}. In addition, the activity of the Cr(III)-grafted TiO_2 photocatalyst was highly reproducible.

1. Introduction

TiO_2 is well-known as an efficient photocatalyst, however, it can only be activated under ultraviolet (UV) light irradiation [1]. Therefore, the effective utilization of visible light has been one of the most important objectives in TiO_2 photocatalyst studies. For this reason, the doping of a foreign element into TiO_2 has been performed since the early 1980s. For example, studies which substitute 3d transition metal ions (Cr, V, Fe, Mn, Co, Ni, etc.) for Ti sites have been performed [2]. In 2001, N-doped TiO_2 in which a nitrogen atom was substituted for a lattice oxygen site was reported as a visible light sensitive photocatalyst, and has attracted a lot of attention [3]. Since that report, TiO_2 doped with various types of anions, such as sulfur, carbon, and iodine, have been widely studied and are very promising candidates for use in practical applications [4]. Most of these doped TiO_2 photocatalysts are sensitive to visible light due to the formation of a localized narrow band in the forbidden band of TiO_2, which originates from the dopant cations and anions.

Recently, we have demonstrated that photocatalytic oxidative decomposition can be initiated by a visible light-induced charge transfer from Cr(III) (or Ce(III)) to the conduction band (CB) of TiO_2 when Cr(III) (or Ce(III)) ions are grafted on the TiO_2 surface (Cr(III)/TiO_2 or Ce(III)/TiO_2) [5]. This process corresponds to a type of interfacial charge transfer (IFCT) between the discrete energy levels of the molecular species and the continuous ones of solids, as predicted by Hush [6] and theoretically formulated by Creutz et al. [7]. In the system, through analogy to the Cu(II)/TiO_2 system, initiated by the IFCT from the valence band (VB) of TiO_2 to Cu(II) [8], we proposed that electrons in Cr(III) ions are directly transferred to the CB of TiO_2, which forms Cr(IV). The electrons in the CB of TiO_2 are then consumed in the reduction of O_2. In contrast, the generated Cr(IV) ions are returned back to the initial Cr(III) ions by extracting electrons from organics, i.e. oxidizing organics (Fig. 1). Subsequently, the system functions catalytically and exhibits oxidative decomposition activity.

As mentioned above, there have been numerous reports regarding the substitution of metal ions at Ti sites [2]. The substitution of metal ions forms a localized narrow band in the forbidden band which originates from the d-orbitals of metal ions [2]. However, the basic concept to obtain visible light sensitivity by

* Corresponding author. Tel.: +81 55 220 8092; fax: +81 55 220 8092.
** Corresponding author at: Research Center for Advanced Science and Technology, The University of Tokyo, 4-6-1 Komaba, Meguro-ku, Tokyo 153-8904, Japan. Tel: +81 3 5452 5080; fax: +81 3 5452 5084.
E-mail address: hirie@yamanashi.ac.jp (H. Irie).

0926-3373/$ – see front matter © 2010 Elsevier B.V. All rights reserved.
doi:10.1016/j.apcatb.2010.02.011

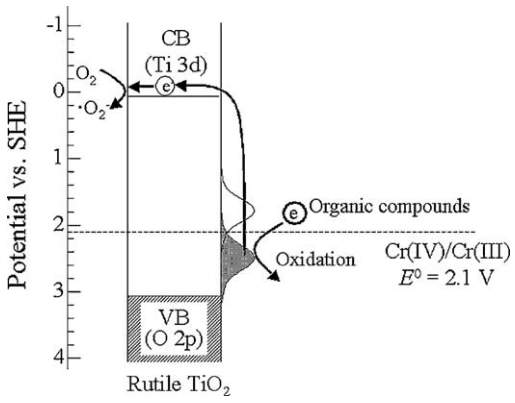

Fig. 1. Proposed mechanism for the generation of photocatalytic activity under visible light. Visible light irradiation induces interfacial charge transfer from the Cr(III) ion to the conduction band of TiO_2.

grafting metal ions on a TiO_2 surface in the present study differs completely from that of substitution at the Ti sites. We hypothesize that metal ion grafting does not form a localized narrow band, and the d-orbitals in the grafted metal ions exist discretely near the TiO_2 surface.

Herein, we report the structural features, including the chemical state and coordination environment of Cr ions, in the Cr(III)/TiO_2 photocatalyst by means of X-ray absorption fine structure (XAFS) technique. In addition, we determined the effect of the amount of grafted Cr(III) on the photocatalytic oxidative activity by gaseous 2-propanol decomposition and the evaluation of oxidative power as revealed by photocurrent measurements.

2. Experimental

2.1. Preparation of Cr(III)/TiO_2

The Cr(III)/TiO_2 photocatalyst was prepared by an identical impregnation method described in our previous report [5], using $CrCl_3{\cdot}6H_2O$ (Aldrich) as the source of Cr(III). One gram of TiO_2 (1.25×10^{-2} mol) powder (rutile form, grain size 15 nm, surface area 90 $m^2\ g^{-1}$, MT-150A, TAYCA) was dispersed in 10 g of distilled water. The amount of $CrCl_3{\cdot}6H_2O$ used corresponded to a weight fraction of Cr relative to TiO_2 of 0–3.0×10^{-3}. The $CrCl_3{\cdot}6H_2O$ was then added to the aqueous TiO_2 suspension, heated at 90 °C and stirred for 1 h in a vial reactor. The suspension was then filtered twice with a membrane filter (0.025 μm, Millipore) and washed with copious amounts of distilled water. The residues were dried at 110 °C for 24 h and subsequently ground into a fine powder using an agate mortar.

2.2. Characterizations

The structural features of the grafted Cr ions in the prepared photocatalyst were characterized by XAFS, including X-ray absorption near-edge structure (XANES) and extended X-ray absorption fine structure (EXAFS). XAFS measurements were performed using the photocatalyst obtained from the weight fraction of Cr/TiO_2 equaling 3.0×10^{-3}. To prepare the samples, 0.5 g of the obtained photocatalyst was dispersed in 1.5×10^{-3} g of distilled water. The suspended solution was then spread on a glass substrate using a rubber squeegee, followed by drying at 110 °C for 5 min. The XAFS spectra for the Cr K-edge were recorded on a beamline 01B01 at SPring-8, which is administered by the Japan Synchrotron Radiation Research Institute (JASRI) [9]. Transmission (Cr_2O_3, CrO_2 and K_2CrO_4) and fluorescence yield (photocatalyst) spectra were acquired using a double-crystal Si(1 1 1) monochromator, ion chambers and a 19-element germanium solid state detector (SSD) equipped with a vanadium filter. The XAFS data were analyzed using the REX2000 (Rigaku Corporation) with theoretical standards given by FEFF8 [10]. UV–vis absorption spectra were obtained by the diffuse reflection method using a spectrometer (UV-2550, Shimadzu).

2.3. Photocatalytic activity

The photocatalytic activity was evaluated by monitoring 2-propanol gas decomposition under visible light irradiation, as described in our previous report [5]. Briefly, visible light (1 mW cm^{-2}, 450–580 nm) from the Xe lamp (Luminar Ace 210, Hayashi Tokei Works) with a combination of glass filters (B-46, Y-47, C-40C, AGC Techno Glass) was used to irradiate the Cr(III)/TiO_2 photocatalysts. Incident-light intensity and wavelength were measured by a spectrometer (Ushio, USR-30). A 300-mg sample was uniformly spread over the irradiation area (~5.5 cm^2) in a 500-mL quartz vessel. The vessel was evacuated and filled with fresh synthetic air. To eliminate organic contaminants on the sample surface, it was illuminated with visible light until the rate of CO_2 generation was less than 0.02 μmol/day. The vessel was then evacuated and filled again with fresh synthetic air, followed by the injection of 6.1 μmol (300 ppm) of the reactant gas. The samples were kept in the dark until the gas concentration became constant, which indicated that the adsorption of 2-propanol gas onto the powder surface was complete. Visible light irradiation was then started, and the concentrations of acetone and CO_2 produced were monitored using a gas chromatograph (model GC-8A, Shimadzu).

To confirm the stability of the photocatalyst obtained from the weight fraction of Cr/TiO_2 equaling 1.0×10^{-3}, when a moderate irradiation time (~100 h) passed, the vessel was evacuated again and refilled with fresh synthetic air. A second 2-propanol decomposition test was then started. Specifically, after eliminating the organic contaminants in the sample and then completing the adsorption of 2-propanol onto the powder surface after injection of 2-propanol (6.1 μmol), visible light irradiation was started. Again, after a moderate irradiation time had passed (~400 h), a third and final cycle was performed.

2.4. Photoelectrochemical measurement

To evaluate the oxidative power of the photocatalyst, the photocurrent was measured using the photocatalyst obtained from the weight fraction of Cr/TiO_2 equaling 1.0×10^{-3}. A film electrode of Cr(III)/TiO_2 was prepared as follows: the Cr(III)/TiO_2 powder was ground and dispersed in distilled water (10 wt% vs. H_2O). The resultant suspension was then applied onto transparent conductive oxide (ITO, Kuramoto, resistance of ~7 Ω sq^{-1}) substrates using a spincoater at 2000 rpm for 6 s, and these were heated at 110 °C. This procedure was repeated twice, and a copper wire was then attached on the edge of the ITO substrate with silver paste. The photocurrent was measured as a function of wavelength (λ) using a monochromatic light source (Sumitomo Heavy Industries Advanced Machinery). The incident photon-to-current conversion efficiency (IPCE/%) was calculated using the following equation:

$$\mathrm{IPCE}(\lambda) = \frac{1240 \times j(\lambda)}{\lambda\, I_0(\lambda)} \times 100$$

where λ is the wavelength of light (nm), $j(\lambda)$ is the photocurrent density (mA cm^{-2}) under illumination at λ, and $I_0(\lambda)$ is the incident-light intensity (mW cm^{-2}) at λ. The photocurrent was measured using a potentiostat (Solartron Instruments, SI1287) in a cell consisting of the prepared films applied on an ITO substrate as the working electrode, Ag/AgCl as the reference electrode, and Pt as the counter electrode in a 0.1 M Na_2SO_4 aqueous solution. Photocurrent measurements with sacrificial reductant (0.5 mM

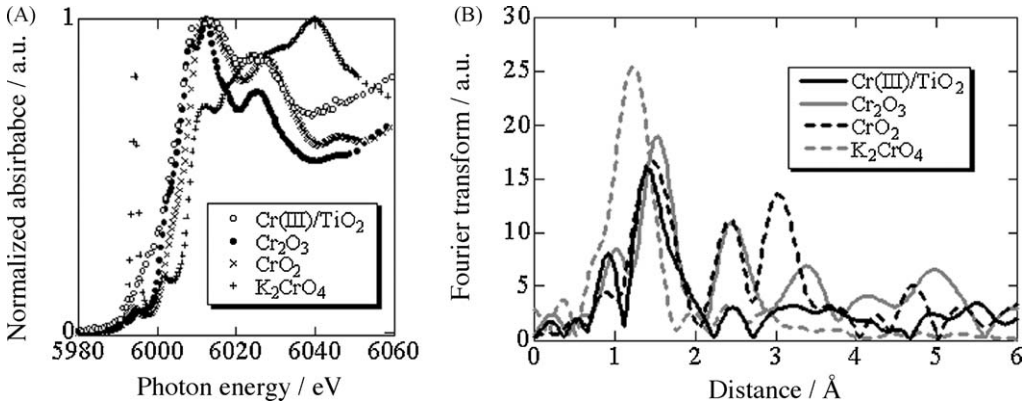

Fig. 2. Cr K-edge XANES spectra of Cr_2O_3, CrO_2 and K_2CrO_4 references and as-prepared Cr(III)/TiO_2 photocatalyst (A). Fourier transforms (FTs) of the $k^3\chi(k)$ EXAFS for the Cr_2O_3, CrO_2 and K_2CrO_4 references and as-prepared Cr(III)/TiO_2 photocatalyst (B).

of KI and KSCN) in 0.1 M $HClO_4$ aq. were conducted to evaluate the oxidation power of the produced Cr(IV) under light irradiation.

3. Results and discussion

3.1. Characterization of Cr(III)/TiO_2

We first determined the Cr K-edge XANES spectra for Cr_2O_3, CrO_2, K_2CrO_4 and the prepared Cr-grafted TiO_2 (Cr ion graft of 3.0×10^{-1} wt%) photocatalyst (Fig. 2A). When compared, it is clear that the spectrum for Cr-grafted TiO_2 resembled that of Cr_2O_3, and was qualitatively different from the spectra obtained for CrO_2 and K_2CrO_4. As there was no detectable Cr(IV) and Cr(VI) in the Cr-grafted TiO_2, we can conclude that the Cr ions were grafted in the 3+ oxidation state (Cr(III)).

The Fourier transforms (FTs) of the $k^3\chi(k)$ EXAFS for the Cr_2O_3, CrO_2 and K_2CrO_4 references and the photocatalyst are shown in Fig. 2B, without phase shift correction. Similar to the XANES results, the FT for the photocatalyst resembled that of Cr_2O_3. In fact, the Cr–O bond length of the photocatalyst (1.966 ± 0.004 Å) obtained by the curve-fitting analysis based on the FEFF standard was very similar to the one of Cr_2O_3 (1.986 ± 0.003 Å), but not to that of CrO_2 (1.906 ± 0.003 Å). Thus, the Cr(III) in the photocatalyst seems to form an amorphous-like Cr_2O_3 clusters and attaches to the TiO_2 surface (Appendix A).

We next subjected the bare rutile TiO_2 and Cr(III)/TiO_2 photocatalysts to UV–vis diffuse reflectance spectroscopy (Fig. 3A). As can been seen from the spectrum, the absorption intensity of TiO_2 began to increase at ~410 nm, which corresponds to the interband transition of rutile TiO_2. This indicates a bandgap of 3.0 eV and is very close to the previously reported value [11]. As for Cr(III)/TiO_2, the spectra showed absorption in the 620-nm region and an absorption shoulder at ~450 nm, in addition to the onset of absorption at ~410 nm. The 620-nm absorption can be assigned to the Cr(III) d–d transition [12]. We have previously ascribed the absorption at ~450 nm of Cr(III)/TiO_2 to the direct IFCT from Cr(III) to the CB of TiO_2 and partly to d–d transition [5,13]. The bold arrow in Fig. 1 shows this charge transfer. The absorption at ~450 nm increased with increasing amounts of Cr(III) in the grafts (Fig. 3A) (Appendix B).

The Δ(1-reflectance) at 450 and 620 nm were calculated by subtracting the (1-reflectance) values at 450 and 620 nm of TiO_2 from those of Cr(III)/TiO_2 and were plotted against the amount of Cr(III) in the photocatalyst (Fig. 3B). The Δ(1-reflectance) at 620 nm increased almost linearly with increasing amounts of Cr(III) in the grafts, which is reasonable as the Δ(1-reflectance) at 620 nm is due to the Cr(III) d–d transition. In contrast, the increase in Δ(1-reflectance) at 450 nm could be divided into two parts. When the amount of Cr(III) was ≤0.06 wt%, the Δ(1-reflectance) increased sharply, but above this wt% (≥0.1%) the increase was similar to that observed at 620 nm. As discussed above, the absorption at ~450 nm is a result of both Cr(III) d–d transition and the IFCT from Cr(III) to the CB of TiO_2, which is the case in the lower Cr(III) wt% region (≤0.06 wt%). However, in the higher wt% region (≥0.1 wt%) the absorption is mainly due to Cr(III) d–d transition with a relatively small contribution from IFCT. We propose that the Cr(III) ions in the lower wt% range are in cluster form and highly dispersed, and thereby actively participate in IFCT. However, as the concentration of Cr(III) ions increases, the clusters begin to aggregate which increases the number of inert ions for IFCT, and explains why the Δ(1-reflectance) curve was not as steep.

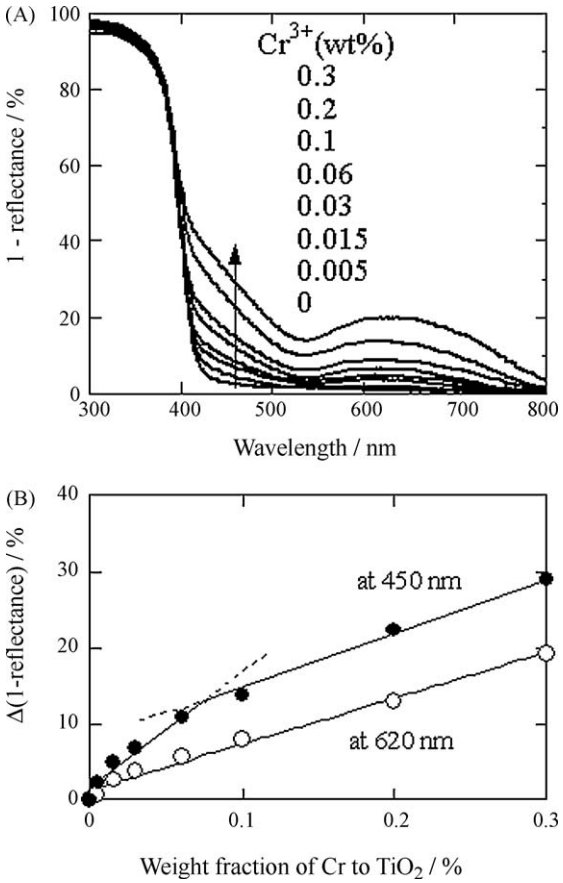

Fig. 3. UV–vis diffuse reflection spectra for Cr(III)/TiO_2 (A). Δ(1-reflectance) vs. weight fractions of Cr to TiO_2 at 450 and 620 nm (B).

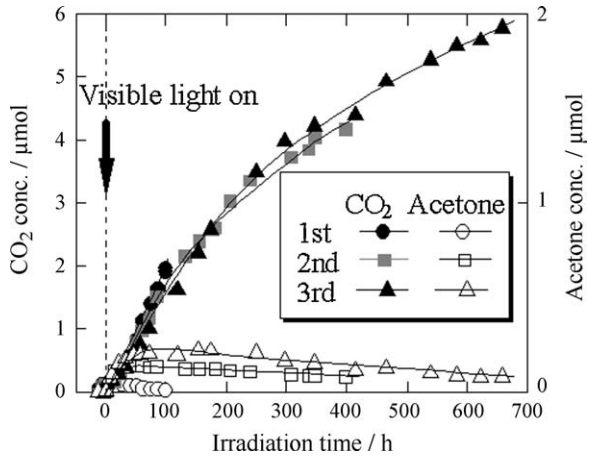

Fig. 4. Changes in acetone and CO_2 concentrations evolved by 2-propanol decomposition as a function of time in the presence of Cr(III)/TiO_2 (0.10 wt%) The decomposition tests were repeated three times.

Table 1
Absorbed photon numbers, CO_2 generation rates and QE values obtained from 2-propanol decomposition tests in the presence of Cr(III)/TiO_2.

Cr(III) grafts (wt%)	Absorbed photon number (quanta cm^{-2} s^{-1})	CO_2 generation rate (pmol s^{-1})	Quantum efficiency (%)
0.005	6.4×10^{13}	1.8	1.9
0.015	1.2×10^{14}	2.9	1.6
0.03	1.4×10^{14}	3.3	1.7
0.06	2.2×10^{14}	6.0	1.8
0.1	2.5×10^{14}	6.3	1.7
0.2	3.6×10^{14}	3.8	0.7
0.3	5.3×10^{14}	3.1	0.4
0.1 (2nd)	2.5×10^{14}	6.1	1.7
0.1 (3rd)	2.5×10^{14}	5.9	1.6

3.2. Photocatalytic activity

The photocatalytic activity of Cr(III)/TiO_2 was determined using a 2-propanol decomposition assay, which evolves acetone and CO_2 under visible light irradiation (Fig. 4). In a typical pattern of acetone and CO_2 evolution for the Cr(III)/TiO_2 photocatalyst (0.10 wt% Cr(III)), the acetone concentrations initially increased and then started to gradually decrease, accompanied by CO_2 production. This profile is plausible, as it is known that 2-propanol decomposes into CO_2, which is the final product, via acetone, the intermediary product [13]. The quantum efficiency (QE) for CO_2 generation was calculated using the formula: QE = 6 × CO_2 generation rate/absorption rate of incident photons; where the CO_2 generation rate was obtained from the slope of the CO_2 generation curve (Fig. 4). The absorption rates of the incident photons, the CO_2 generation rates, and QEs for all of the photocatalysts were calculated and compared (Table 1). When the amount of Cr(III) increased from 0 to 0.06–0.1 wt%, the CO_2 generation rate increased while the QE values remained constant. This can be explained as follows: the Cr(III) ions in cluster form are highly dispersed in the 0.03–0.1 wt% range as described above and illustrated in Fig. 3B. Since the clusters are active to IFCT and are independent of one another, the QE was maintained at a constant value. Thus, the CO_2 generation rates were determined by the visible light-absorption originating from IFCT, and the photon absorption capability increased with increasing amounts of Cr(III). Further increasing the amount of Cr(III) in the grafts (>0.1 wt%), resulted in a decrease of both the CO_2 generation rates and QE values (Table 1). This might be explained by the "quenching" of the generated electrons and Cr(IV), as the recombination possibility of the generated electrons and Cr(IV) will increase before oxygen is reduced by electrons and 2-propanol is oxidized by Cr(IV).

To examine the reproducibility of the photocatalytic activity of Cr(III)/TiO_2 we twice repeated the 2-propanol decomposition assay (Fig. 4 and Table 1). It should be noted that the acetone and CO_2 generation behaviors were quite similar among the three photocatalytic decomposition tests. In addition, the CO_2 generation rate and QE values were within experimental error among these three tests, indicating that the Cr(III)/TiO_2 photocatalyst is stable under these light conditions for approximately 1200 h (total irradiation time).

3.3. Photoelectrochemical measurement

The changes in IPCE for the Cr(III)/TiO_2 film (0.1 wt% graft) in the absence and presence of sacrificial reductants (KI, KSCN) in 0.1 M $HClO_4$ aq. electrolyte solution were determined (Fig. 5A and B). In the absence of sacrificial reductants, a photocurrent was observed for the film when irradiated with visible light with a wavelength less than 480 nm, indicating the visible light sensitivity of the Cr(III)/TiO_2 film (Fig. 5B). When irradiated with visible light in the presence of sacrificial reductants, an increase of IPCE was observed only by the addition of I^- ($E^0(I^\bullet/I^-)$ = 1.35 V) and not by the addition of SCN^- ($E^0(SCN^\bullet/SCN^-)$ = 1.64 V). In contrast, when irradiated with light (<420 nm) that can be absorbed by the interband transition of rutile TiO_2, the IPCE increased when either of the sacrificial reductants was added.

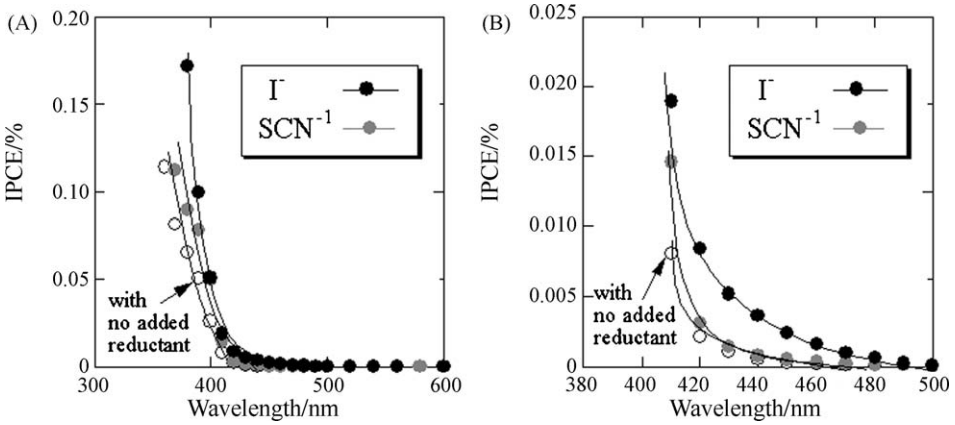

Fig. 5. Effect of the addition of reductants (I, SCN) on IPCE spectra for the Cr(III)/TiO_2 electrode with a Cr graft of 0.01 wt% (A). (B) is the enlargement of (A) in the visible light region.

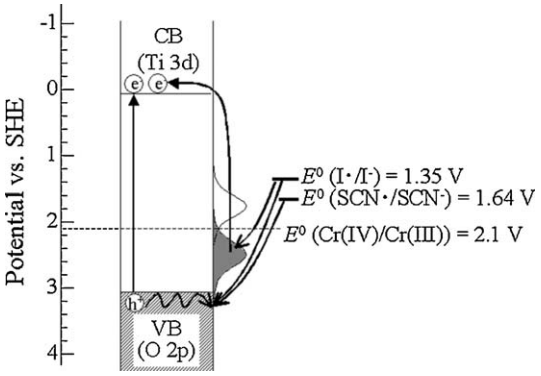

Fig. 6. Schematic illustration of the energy diagram together with photo-induced IFCT and bandgap excitation. The equilibrium redox potentials for the one-electron-transfer redox couples (E^0) are indicated.

To explain this result, we must consider the potential of the Cr(IV)/Cr(III) redox couple (E^0 = 2.1 V) and the sacrificial reductant. As the Cr(IV) generated by visible light-induced IFCT contributes to oxidation, according to our proposed mechanism for the visible light sensitivity of Cr(III)/TiO_2, it can be expected that the more negative the redox potential of a reductant, the more easily it is oxidized. This is the case for $I^{\bullet}/I^-$ as its redox potential is more negative than Cr(IV)/Cr(III), suggesting that I^- can be easily oxidized by Cr(IV), which is in agreement with the present result (Fig. 6). However, we have no clear explanation for the low reactivity in the presence of SCN^-, even though its redox potential is more negative than Cr(IV)/Cr(III). It can possibly be attributed to the presence of large reorganization energies in the electron-transfer reaction for such small ions in aqueous solution [14]. Both I^- and SCN^- ions are small, so even though both I^- and SCN^- ions have large reorganization energies, it might be possible that only I^- could be oxidized by Cr(IV) but SCN^- could not, because the redox potential of $I^{\bullet}/I^-$ is more negative than that of $SCN^{\bullet}/SCN^-$. Under light irradiation which can induce bandgap transition (<420 nm in the present study), holes in the VB of rutile TiO_2 formed by interband transition can oxidize both I^- and SCN^- (Fig. 6). A similar observation was also reported for nitrogen-doped anatase TiO_2 [14,15]. Under UV light irradiation, which can induce bandgap transition of anatase (<385 nm), both I^- and SCN^- were oxidized. In contrast, visible light irradiation with wavelengths of ~400–500 nm resulted in the oxidation of only I^-. In nitrogen-doped TiO_2, the isolated narrow band composed of N 2p is formed 0.75 eV above the VB of TiO_2 (2.25 V (vs. SHE)) which is close to the E^0 of Cr(IV)/Cr(III) (2.1 V). It is well-known that the isolated N 2p band contributes to visible light sensitivity, therefore we can confidently conclude that the produced Cr(IV) plays a role in the visible light sensitivity observed in this study.

Finally, we compared the present Cr(III)/TiO_2 system to Cr(III) ion doped TiO_2 photocatalyst [2]. Cr(III) substitution at a Ti(IV) site, which differs from surface modification, forms a localized narrow band derived from the Cr 3d orbital in the forbidden band. In this case, the photo-generated holes must diffuse through the localized narrow band to the surface in order to react with adsorbents. Typically, the localized narrow band has a small-dispersed density of states (DOSs). Additionally, distortion might be introduced into the TiO_2 lattice due to the mismatch of the ionic radii between Cr(III) (0.0615 nm) and Ti(IV) (0.0605 nm). Thus, the mobility of holes induced by visible light in the Cr-doped TiO_2 might be small, which is unfavorable for photocatalytic activity. In contrast, the Cr 3d orbitals are dispersed on the TiO_2 surface in the present Cr(III)/TiO_2 system, and the photo-generated holes do not need to diffuse. This represents a favorable factor for the photocatalytic activity under visible light in the presence of Cr(III)/TiO_2.

4. Conclusions

Using the Cr K-edge XAFS spectra, we determined that the grafted Cr species in the Cr(III)/TiO_2 photocatalyst are actually in the 3+ state, have an Cr_2O_3-like conformation, and form clusters. In addition, such Cr(III) grafts onto TiO_2 could produce a stable photocatalyst under visible light irradiation. As the IFCT proceeds between Cr(III) and the CB of TiO_2, it is preferable that the Cr(III) ions are atomically isolated on the TiO_2 surface. Therefore, Cr(III) ions should be grafted as mononuclear Cr(III) in order to improve the efficiency of IFCT and enhance the photocatalytic activity. In addition, obtaining the direct evidence of the electron transfer from Cr(III) to CB of TiO_2 is very important. Such investigations are now underway in our laboratory.

Acknowledgements

The X-ray absorption fine structure (XAFS) measurements were performed at the SPring-8 with approval of the Japan Synchrotron Radiation Research Institute (JASRI) (Proposal No. 2008A1048). We are grateful to Dr. H. Tanida for help on the measurements of XAFS spectra. This work was performed under the management of Project to Create Photocatalyst Industry for Recycling-oriented Society supported by NEDO (New Energy and Industrial Technology Development Organization). We express gratitude to Mr. G. Newton for the careful reading of the manuscript.

Appendix A

The Cr–Cr bond length could not be analyzed quantitatively because of low signal intensity.

Appendix B

Elemental analyses of the prepared Cr(III)/TiO_2 photocatalyst, obtained from weight fraction of only $Cr/TiO_2 = 1.0 \times 10^{-3}$, were performed using an inductively coupled plasma atomic emission spectrometer (ICP-AES, P-4010, Hitachi) for Ti and a polarized Zeeman atomic absorption spectrophotometer (Z-2000, Hitachi) for Cr. The analyses indicated that the weight fraction of Cr relative to TiO_2 was 1.0×10^{-3}, exactly equal to the starting ratio used in the preparation. By the analogy with the previous reported Cu(II)/TiO_2 [8], the weight fractions of Cr relative to TiO_2 in the photocatalysts were nearly equal to the starting ratio used in the preparation up to $Cr/TiO_2 = 3.0 \times 10^{-3}$.

References

[1] H. Gerischer, A. Heller, J. Electrochem. Soc. 139 (1992) 113–118;
A.L. Linsebigler, G.Q. Lu, J.T. Yates, Chem. Rev. 95 (1995) 735–758;
M.R. Hoffmann, S.T. Martin, W. Choi, D.W. Bahnemann, Chem. Rev. 95 (1995) 69–96.
[2] E. Borgarello, J. Kiwi, M. Grätzel, E. Pelizzetti, M. Visca, J. Am. Chem. Soc. 104 (1982) 2996–3002;
J.-M. Herrmann, J. Dissier, P. Pichat, Chem. Phys. Lett. 108 (1984) 618–622;
H. Yamashita, Y. Ichihashi, M. Takeuchi, S. Kishiguchi, M. Anpo, J. Synchrotron Radiat. 6 (1999) 451–452;
M. Anpo, M. Takeuchi, J. Catal. 216 (2003) 505–516;
T. Umebayashi, T. Yamaki, H. Itoh, K. Asai, J. Phys. Chem. Solids 63 (2002) 1909–1920.
[3] R. Asahi, T. Morikawa, T. Ohwaki, K. Aoki, Y. Taga, Science 293 (2001) 269–271.
[4] H. Irie, Y. Watanabe, K. Hashimoto, J. Phys. Chem. B 107 (2003) 5483–5486;
T. Umebayashi, T. Yamaki, H. Itoh, K. Asai, Appl. Phys. Lett. 81 (2002) 454–456;
T. Umebayashi, T. Yamaki, S. Tanaka, K. Asai, Chem. Lett. 32 (2003) 330–331;
T. Ohno, M. Akiyoshi, T. Umebayashi, K. Asai, T. Mitsui, M. Matsumura, Appl. Catal. A 265 (2004) 115–121;
T. Ohno, T. Mitsui, M. Matsumura, Chem. Lett. 32 (2003) 364–365;
H. Irie, S. Washizuka, K. Hashimoto, Thin Solid Films 510 (2006) 21–25;
S. Sakthivel, H. Kisch, Angew. Chem. Int. Ed. 42 (2003) 4908;
H. Irie, S. Washizuka, K. Hashimoto, Chem. Commun. 11 (2003) 1298–1299;
H. Irie, S. Washizuka, Y. Watanabe, T. Kako, K. Hashimoto, J. Electrochem. Soc. 152

(2005) E351–E356;
M. Mrowetz, W. Balcerski, M.R. Hoffmann, J. Phys. Chem. B 108 (2004) 17269–17273.
[5] H. Irie, S. Miura, R. Nakamura, K. Hashimoto, Chem. Lett. 37 (2008) 252–253; R. Nakamura, A. Okamoto, H. Osawa, H. Irie, K. Hashimoto, J. Am. Chem. Soc. 129 (2007) 9596–9597.
[6] N.S. Hush, J. Electroanal. Chem. 470 (1999) 170–195.
[7] C. Creutz, B.S. Brunschwig, N. Sutin, J. Phys. Chem. B 109 (2005) 10251–10260; C. Creutz, B.S. Brunschwig, N. Sutin, J. Phys. Chem. B 110 (2006) 25181–25190.
[8] H. Irie, K. Kamiya, S. Miura, K. Hashimoto, Chem. Phys. Lett. 457 (2008) 202–203; H. Irie, K. Kamiya, T. Shibanuma, S. Miura, D.A. Tryk, T. Yokoyama, K. Hashimoto, J. Phys. Chem. C. 113 (2009) 10761–10766.
[9] T. Uruga, H. Tanida, Y. Yoneda, K. Takeshita, S. Emura, M. Takahashi, M. Harada, Y. Nishihata, Y. Kubozono, T. Tanaka, T. Yamamoto, H. Maeda, O. Kamishima, Y. Takabayashi, Y. Nakata, H. Kimura, S. Goto, T. Ishikawa, J. Synchrotron Radiat. 6 (1999) 143–145.
[10] E.A. Stern, M. Newville, B. Ravel, T. Yacoby, D. Haskel, Physica B 209 (1995) 117–120.
[11] T. Torimoto, N. Nakamura, S. Ikeda, B. Ohtani, Phys. Chem. Chem. Phys. 4 (2002) 5910–5914.
[12] A.J. McCaffery, P.J. Stephens, P.N. Schatz, Inorg. Chem. 6 (1967) 1614–1625.
[13] Y. Ohko, K. Hashimoto, A. Fujishima, J. Phys. Chem. B 101 (1997) 8057–8062.
[14] R. Nakamura, T. Tanaka, Y. Nakato, J. Phys. Chem. B 108 (2004) 10617–10620.
[15] K. Obata, H. Irie, K. Hashimoto, Chem. Phys. 339 (2007) 124–132.